

Parallel Group Detection Approach for Massive MIMO systems

Thanh-Binh Nguyen, Minh-Tuan Le

Le Quy Don Technical University

236 Hoang Quoc Viet, Cau Giay, Ha Noi, Vietnam

email: nguyenthambinhstt@gmail.com

MobiFone R&D Center, MobiFone Corporation

VP1 Lot, Yen Hoa Ward, Cau Giay Dist., Hanoi, Vietnam

e-mail: tuan.minh@mobifone.vn

Vu-Duc Ngo, Van-Giao Nguyen

Hanoi University of Science and Technology

01 Dai Co Viet street, Hai Ba Trung Dist., Hanoi, Vietnam

e-mail: duc.ngovu@hust.edu.vn

Le Quy Don Technical University

236 Hoang Quoc Viet, Cau Giay, Ha Noi, Vietnam

email: giaonv@mta.edu.vn

Abstract—In this paper, we develop a new detection algorithm, called Parallel Group Detection (PGD), which enables the classical detectors to improve Bit Error Rate (BER) performance of Massive MIMO systems. In the algorithm, the Massive MIMO system equation is converted into an extended form and divided to provide two sub-systems, which can subsequently be detected by the classical detectors to recover transmitted signals. Based on the PGD, the conventional QRD and SQRD detectors, we propose two efficient detectors, called QRD based PGD (QRD-PGD) and Sorted QRD based PGD (SQRD-PGD). Numerical and simulation results for different antenna configurations show that the proposed detectors can achieve a gain of more than 4 dB in BER performance as compared to that of the Minimum Mean Square Error (MMSE) one while their computational costs are comparable.

Index Terms—Massive MIMO, Parallel Group Detection, Linear Detector, QR decomposition, Successive Interference Cancellation.

I. INTRODUCTION

In recent years, Massive Multiple Input Multiple Output (Massive MIMO) systems have attracted the interest of many researchers all over the world. By using hundreds of antennas at the Base Station (BS) to simultaneously serve dozens of multiple-antenna-users, Massive MIMO can provide not only very high spectral efficiency but also but also high energy efficiency [1]–[4].

In the up-link scenario, signals from active users are transmitted through a wireless medium to the BS. At the BS, the signals need to be recovered reliably via the use of suitable detectors. Typically, the number of antennas equipped at the BS is much larger than that of all activated users. This leads to very low load factor, which is defined by the ratios of total transmit antennas and receive ones. In such scenarios, linear detectors, such as Matched Filter (MF), Zero Forcing (ZF) or Minimum Mean Square Error (MMSE) can provide nearly optimal Bit Error Rate (BER) performances [2]. In [5] the authors showed that QR decomposition based detector (QRD) and Sorted QRD (SQRD) are suitable for Massive MIMO systems when the channel coefficients are correlated. In [4] the ZF-GD and ZF-IGD (ZF based Iterative Group Detection) detectors based on the Group Detection (GD) concept were

proposed. The ZF-IGD was shown to outperform both the ZF and MMSE detectors at the cost of slightly higher detection complexity. Unfortunately, at high load factors, the ZF-GD and ZF-IGD detectors suffer from performance loss and noticeably underperform the MMSE one.

In [6] the authors pointed out that there is no strict requirement on the relation between the number of antenna equipped at the BS and the number of users. This means that Massive MIMO system can be defined unconventionally as large number of BS antenna to serve very large number of users simultaneously. In reality, it is desirable to maximize the number of users served by the BS at a time. Thus, it is of necessity to develop high-performance detectors for Massive MIMO systems under high load condition, especially as the load factor approaches unity.

High performance detectors such as the Maximum Likelihood (ML) detector and Sphere Detector (SD) can be used to address the issue of high load condition. Nevertheless, these detectors require huge amount of computational resources, thereby preventing them from being adopted in practice. Similarly, other conventional detectors, such as Bell Laboratory Space Time (BLAST) [7] or Lattice Reduction (LR) aided detectors, can not be applied directly. To overcome the problem, the Local Ascent Search (LAS) and Random Tabu Search (RTS), proposed for very large MIMO systems in [8], can be considered in Massive MIMO scenario. Other way of improving the performance of the conventional detectors is to use the Spare Error Recovery approach, which was presented in [9].

In this paper, we propose a Parallel Group Detection (PGD) algorithm so as to improve BER performance of classical detectors when they are used in high-load Massive MIMO systems. In the proposed approach, the Massive MIMO system equation is first converted into an extended form and divided into two sub-systems. After that conventional detectors are applied to the sub-systems to recover the transmit signals in a parallel fashion. Based on the PGD as well as the conventional QRD and SQRD detectors, we develop two complexity-efficient and high performance detectors, called QRD based PGD (QRD-PGD) and Sorted QRD based PGD

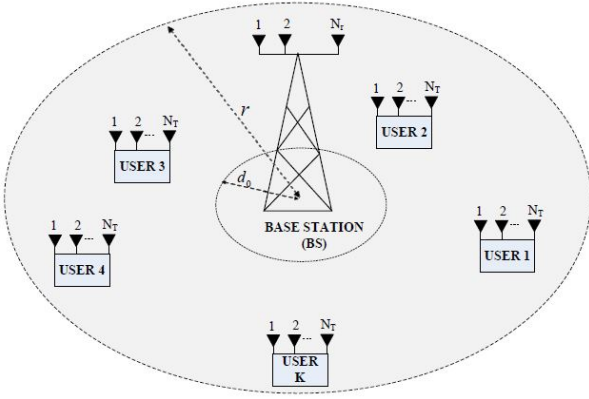


Fig. 1. Up-link Massive MIMO system model

(SQRD-PGD). Numerical and simulation results demonstrate that the proposed detectors remarkably outperform various existing detectors at comparable complexity levels.

The rest of the paper is presented as follows. Section II shows an up-link model of a Massive MIMO system. The PGD algorithm and the proposed detectors are described in Section III. Section IV and Section V respectively presents BER performance comparison and complexity analysis. Finally, the conclusions are drawn in Section VI.

Notations: $\mathbf{A}(:, l : k)$ is taking l th to k th columns of matrix \mathbf{A} while $\mathbf{b}(l : k)$ denotes the taking of l th to k th elements of column vector \mathbf{b} ; $(\cdot)^T$ and $(\cdot)^H$ are transpose and Hermitian transpose of a matrix or vector; $E[\cdot]$ and \otimes denote expectation operation and Kronecker product, respectively; \mathbf{A}^\dagger is pseudo inverse of matrix \mathbf{A} (i.e. $\mathbf{A}^\dagger = (\mathbf{A}^H \mathbf{A})^{-1} \mathbf{A}^H$).

II. SYSTEM MODEL

Consider an up-link scenario of a single cell Massive MIMO system as illustrated in Fig. 1. The Base Station is assumed to be located at the origin of the circular cell with radius r and reference distance d_0 . All users are located randomly in the cell such that $d_0 \leq d_k \leq r$, where d_k is the distance from k th user to the BS. The BS equipped with N_r receive antennas simultaneously serves K multi-antennas users. The received signals at the BS can be expressed as follows:

$$\mathbf{y} = \sqrt{\frac{p_u}{N_T E_s}} \bar{\mathbf{U}} \mathbf{x} + \mathbf{n}, \quad (1)$$

where $\mathbf{y} \in \mathbb{C}^{N_r \times 1}$, $\bar{\mathbf{U}} \in \mathbb{C}^{N_r \times N}$ and $\mathbf{n} \in \mathbb{C}^{N_r \times 1}$ are the received signal vector, the channel matrix, and the noise vector, respectively; N_T and N respectively denote number of antennas placed at each user and total transmit antennas from K users (i.e. $N = KN_T$); E_s is the average symbol energy of M -QAM signals. Assuming that all users have the same transmit power (p_u) and the transmit power of each user is divided equally among N_T transmit antennas, i.e., $E[\mathbf{x}\mathbf{x}^H] = E_s \mathbf{I}_N$. It is further assumed that the entries of \mathbf{n} are i.i.d¹ random variables with zero mean and variance

¹independent identical distributed

$\sigma_n^2 = 1$. Generally, the entries of $\bar{\mathbf{U}}$ can be illustrated by the product of large scaled fading (shadowing and path loss) and small scaled fading coefficients. Therefore, $\bar{\mathbf{U}}$ can be modeled as the following expression [10]:

$$\bar{\mathbf{U}} = \mathbf{H} \mathbf{D}^{1/2}. \quad (2)$$

In (2), $\mathbf{H} \in \mathbb{C}^{N_r \times N}$ is the matrix, whose entries represents small scaled fading coefficients and they can be assumed to be $\mathcal{N}(0, 1)$ i.i.d random variables; \mathbf{D} is a $N \times N$ diagonal matrix where its diagonal elements represent large scale fading coefficients. The large scale fading coefficients from the antennas of k th user to the BS is assumed to be identical because the distances between the antennas placed at each user are much smaller than those between the users and the BS. Hence, the channel matrix $\bar{\mathbf{U}}$ is further represented as:

$$\bar{\mathbf{U}} = \mathbf{H} (\mathbf{B} \otimes \mathbf{I}_{N_T})^{1/2}, \quad (3)$$

where \mathbf{B} is $K \times K$ diagonal matrix with the k th entry at the main diagonal, $b_{k,k}$, representing the large scaled fading coefficients between k th user and the BS. Let z_k be the variance of shadowing from k th user to the BS and γ_p denotes path loss factor. Then $b_{k,k}$ can be calculated using $b_{k,k} = \frac{z_k}{(d_k/d_0)^{\gamma_p}}$ [11].

For simplicity, Let us define $\mathbf{U} = \sqrt{\frac{p_u}{N_T E_s}} \bar{\mathbf{U}}$. Then equation (1) can be rewritten as:

$$\mathbf{y} = \mathbf{U} \mathbf{x} + \mathbf{n}, \quad (4)$$

Equation (4) can be represented in the following extended form [12]:

$$\mathbf{y}_{\text{ex}} = \mathbf{U}_{\text{ex}} \mathbf{x} + \mathbf{n}_{\text{ex}}, \quad (5)$$

where $\mathbf{y}_{\text{ex}} = [\mathbf{y}^T \quad \mathbf{0}_N^T]^T$; $\mathbf{U}_{\text{ex}} = [\mathbf{U}^T \quad \sqrt{\frac{1}{E_s}} \mathbf{I}_N]^T$ and $\mathbf{n}_{\text{ex}} = [\mathbf{n}^T \quad -\sqrt{\frac{1}{E_s}} \mathbf{x}^T]^T$ are the $(N_r + N) \times 1$ extended received vector, $(N_r + N) \times N$ extended channel matrix and $(N_r + N) \times 1$ extended noise vector, correspondingly.

III. PARALLEL GROUP DETECTION AIDED DETECTORS

A. Proposed Parallel Group Detection Algorithm

In general, the extended system (6) can be divided into l sub-systems, where l is an integer satisfying $2 \leq l \leq N$. However, the more sub-systems are created, the higher complexity the detection will be. Therefore, in this paper, we set $l = 2$ in order to keep the complexity at the lowest level. The block diagram of the system using the PGD algorithm with 2 parallel sub-systems is shown in Fig. 2.

Let us assume that the number of users in the sub-system equals to each other and equals to $L = \frac{N}{2}$. In addition, without loss of generality, it is assumed that K is an even number. Under the above assumptions, equation (5) can be rewritten as:

$$\mathbf{y}_{\text{ex}} = \mathbf{G}^{(1)} \mathbf{s}^{(1)} + \mathbf{G}^{(2)} \mathbf{s}^{(2)} + \mathbf{n}_{\text{ex}}, \quad (6)$$

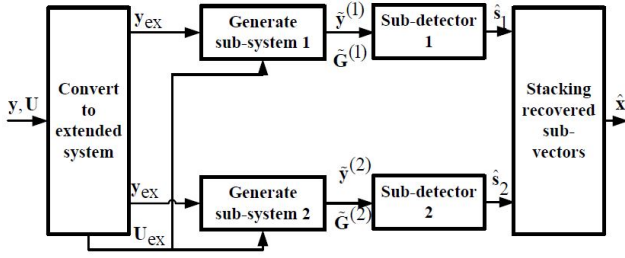


Fig. 2. Block diagram of the system using the PGD algorithm

where both $\mathbf{G}^{(1)}$ and $\mathbf{G}^{(2)}$ are $(N_r + N) \times L$ sub-matrices defined by $\mathbf{G}^{(1)} = \mathbf{U}_{\text{ex}}(:, 1:L)$, $\mathbf{G}^{(2)} = \mathbf{U}_{\text{ex}}(:, L+1:N)$. Similarly, $\mathbf{s}^{(1)} = \mathbf{x}(1:L)$ and $\mathbf{s}^{(2)} = \mathbf{x}(L+1:N)$ are transmitted sub-vectors.

In order to create the 1st sub-system, the interference term $\mathbf{G}^{(2)}\mathbf{s}^{(2)}$ in (6) need to be canceled out. Thanks to the pseudo-inverse projection property², multiplying both side of (6) by $\mathbf{A}^{(1)} = (\mathbf{I} - \mathbf{G}^{(2)}\mathbf{G}^{(2)\dagger})$ we obtain:

$$\mathbf{A}^{(1)}\mathbf{y}_{\text{ex}} = \mathbf{A}^{(1)}\mathbf{G}^{(1)}\mathbf{s}^{(1)} + \mathbf{A}^{(1)}\mathbf{n}_{\text{ex}}. \quad (7)$$

Define $\tilde{\mathbf{y}}^{(1)} = \mathbf{A}^{(1)}\mathbf{y}_{\text{ex}}$, $\tilde{\mathbf{G}}^{(1)} = \mathbf{A}^{(1)}\mathbf{G}^{(1)}$ and $\tilde{\mathbf{n}}^{(1)} = \mathbf{A}^{(1)}\mathbf{n}_{\text{ex}}$ as the respective received vector, channel matrix and noise vector of the 1st sub-system. Equation (7) can be rewritten as:

$$\tilde{\mathbf{y}}^{(1)} = \tilde{\mathbf{G}}^{(1)}\mathbf{s}^{(1)} + \tilde{\mathbf{n}}^{(1)}. \quad (8)$$

Similarly, using the projection term $\mathbf{A}^{(2)} = (\mathbf{I} - \mathbf{G}^{(1)}\mathbf{G}^{(1)\dagger})$ in order to cancel the interference of $\mathbf{G}^{(1)}\mathbf{s}^{(1)}$ in (6), the 2nd sub-system is generated as:

$$\tilde{\mathbf{y}}^{(2)} = \tilde{\mathbf{G}}^{(2)}\mathbf{s}^{(2)} + \tilde{\mathbf{n}}^{(2)}, \quad (9)$$

where $\tilde{\mathbf{y}}^{(2)} = \mathbf{A}^{(2)}\mathbf{y}_{\text{ex}}$, $\tilde{\mathbf{G}}^{(2)} = \mathbf{A}^{(2)}\mathbf{G}^{(2)}$ and $\tilde{\mathbf{n}}^{(2)} = \mathbf{A}^{(2)}\mathbf{n}_{\text{ex}}$ are respectively the received vector, channel matrix and noise vector of the 2nd sub-system.

Now, the transmitted sub-vectors can be easily estimated by applying some conventional detector in a parallel manner. Finally, by stacking the recovered sub-vectors, we obtain the overall estimated vector as $\hat{\mathbf{x}} = \begin{bmatrix} \hat{\mathbf{s}}^{(1)} \\ \hat{\mathbf{s}}^{(2)} \end{bmatrix}$. The PGD algorithm is summarized in Algorithm 1.

It is worthy noting that the channel matrices' dimensions of both the sub-systems are $(N_r + N) \times (N/2)$, which provide much higher degree of freedom and lower β than those of the original system. Hence, the BER performance of sub-systems are improved significantly, as illustrated later. However, the noise terms $\tilde{\mathbf{n}}^{(1)}$ and $\tilde{\mathbf{n}}^{(2)}$ are altered because their co-variances respectively are $E[\tilde{\mathbf{n}}^{(1)}\tilde{\mathbf{n}}^{(1)H}] = (\mathbf{I} - \mathbf{G}^{(2)}\mathbf{G}^{(2)\dagger})(\mathbf{I} - \mathbf{G}^{(2)}\mathbf{G}^{(2)\dagger})^H$ and $E[\tilde{\mathbf{n}}^{(2)}\tilde{\mathbf{n}}^{(2)H}] = (\mathbf{I} - \mathbf{G}^{(1)}\mathbf{G}^{(1)\dagger})(\mathbf{I} - \mathbf{G}^{(1)}\mathbf{G}^{(1)\dagger})^H$. This will degrade BER

² $(\mathbf{I} - \mathbf{A}\mathbf{A}^\dagger)\mathbf{A} = 0$

performance of a detector based on PGD if these noise terms are not considered properly.

Algorithm 1 PGD Algorithm

 Input: $\mathbf{y}, \mathbf{U}, K, N_T$

 Output: $\hat{\mathbf{x}}$

- 1: Convert system to equivalent extended form as $\mathbf{y}_{\text{ex}} = [\mathbf{y}^T \quad \mathbf{0}_N^T]^T$; $\mathbf{U}_{\text{ex}} = [\mathbf{U}^T \quad \sqrt{\frac{1}{E_s}}\mathbf{I}_N]^T$.
 - 2: Set $L = \frac{N}{2}$ and define the channel sub-matrices as $\mathbf{G}^{(1)} = \mathbf{U}_{\text{ex}}(:, 1:L)$, $\mathbf{G}^{(2)} = \mathbf{U}_{\text{ex}}(:, L+1:N)$.
 - 3: Compute projection terms: $\mathbf{A}^{(1)} = (\mathbf{I} - \mathbf{G}^{(2)}\mathbf{G}^{(2)\dagger})$ and $\mathbf{A}^{(2)} = (\mathbf{I} - \mathbf{G}^{(1)}\mathbf{G}^{(1)\dagger})$.
 - 4: Generate two sub-systems in parallel, where their equivalent received vectors and channel matrices are defined as:

$$\tilde{\mathbf{y}}^{(1)} = \mathbf{A}^{(1)}\mathbf{y}_{\text{ex}}, \tilde{\mathbf{G}}^{(1)} = \mathbf{A}^{(1)}\mathbf{G}^{(1)}, \tilde{\mathbf{y}}^{(2)} = \mathbf{A}^{(2)}\mathbf{y}_{\text{ex}}, \tilde{\mathbf{G}}^{(2)} = \mathbf{A}^{(2)}\mathbf{G}^{(2)}.$$
 - 5: Estimate both transmitted sub-vectors $\hat{\mathbf{s}}^{(k)}$, ($k = 1, 2$), by applying suitable detectors to each sub-system.
 - 6: Stacking recovered sub-vectors as $\hat{\mathbf{x}} = [\hat{\mathbf{s}}_1^T \quad \hat{\mathbf{s}}_2^T]^T$.
-

B. Proposed QRD-PGD and SQRD-PGD detectors

Basically, any classical MIMO detector can be adopted for signal recovery in the sub-systems. However, taking performance and complexity into consideration, in Step 5 of Algorithm 1, we apply the QRD and Sorted QRD detectors to obtain the so-called QRD-PGD and SQRD-PGD detectors.

1) *QRD-PGD Detector*: In this method, the transmitted signals on two branches (see Fig. 2) are simultaneously recovered using the conventional QRD detector. The details of the detection process is described as follows.

Using QR decomposition (which can be found in [13]) to decompose the sub-channel matrices $\tilde{\mathbf{G}}^{(k)}$, $k = 1, 2$, we get:

$$\tilde{\mathbf{G}}^{(k)} = \mathbf{Q}^{(k)}\mathbf{R}^{(k)}, \quad (10)$$

where $\mathbf{Q}^{(k)}$ is $(N_r + N) \times L$ unitary matrix (i.e $\mathbf{Q}^{(k)H}\mathbf{Q}^{(k)} = \mathbf{I}$) and $\mathbf{R}^{(k)}$ denotes $L \times L$ upper triangle matrix.

Multiplying both sides of (8) and (9) by $\mathbf{Q}^{(k)H}$ we get

$$\mathbf{v}^{(k)} = \mathbf{Q}^{(k)H}\tilde{\mathbf{y}}^{(k)} = \mathbf{R}^{(k)}\mathbf{s}^{(k)} + \mathbf{Q}^{(k)H}\tilde{\mathbf{n}}^{(k)}. \quad (11)$$

Finally, the transmitted symbols are estimated symbol by symbol using the following rule:

$$\hat{s}_i^{(k)} = \mathfrak{Q}\left(\tilde{s}_i^{(k)}\right) = \mathfrak{Q}\left(\left(v_i^{(k)} - \sum_{j=i+1}^L r_{ij}^{(k)}\hat{s}_j^{(k)}\right) / r_{ii}^{(k)}\right), \quad (12)$$

where $\hat{s}_i^{(k)}$, $i = L, L-1, \dots, 1$, denotes the estimated symbol, $\mathfrak{Q}(\bullet)$ denotes the quantization operator, $v_i^{(k)}$ is i th entries of $\mathbf{v}^{(k)}$, $r_{ij}^{(k)}$ denotes (i th, j th) entries of $\mathbf{R}^{(k)}$.

2) *SQRD-PGD*: It is noteworthy that in the QRD-PGD, the L th symbol is always recovered first. Then it is used to cancel its interference for the detection of subsequent symbols. Hence, if the L th symbol is not the strongest signal (i.e., the symbol corresponds to the strongest channel gain), the BER performance of system will be degraded. By using the classical SQRD [14] as a detector in the PGD, the strongest symbol will be detected first. Therefore, BER performance given by SQRD-PGD is better than that of QRD-PGD one.

In the SQRD-PGD, the channel sub-matrices, $\tilde{\mathbf{G}}^{(k)}$, $k = 1, 2$, are first decomposed to generate the matrices $\mathbf{Q}^{(k)}$, $\mathbf{R}^{(k)}$ and the permutation vectors $\mathbf{p}^{(k)}$. After that the transmitted signals are recovered in exactly the same steps as the QRD-PGD detector. Finally, the estimated signals are resorted as

$$\hat{\mathbf{s}}^{(k)} = \hat{\mathbf{s}}^{(k)}(\mathbf{p}^{(k)}), \quad (13)$$

where $\mathbf{b}(\mathbf{p}^{(k)})$ denotes sorted operation, which rearranges the rows of \mathbf{b} in the same order of $\mathbf{p}^{(k)}$.

IV. BER PERFORMANCE COMPARISON

In this section, BER performances of the proposed detectors are compared to those of classical linear detectors, including QRD, SQRD and MMSE-BLAST (referred to as BLAST in this paper) ones. The simulation parameters are set as follows. Cell radius and reference distance are $r = 1000$ meters and $d_0 = 100$ meters, respectively; All users are assumed to locate randomly in the cell such that the distance from the k th user to the BS satisfying $200\text{ m} \leq d_k \leq 990\text{ m}$. In addition, the distances are unchanged within the channel coherent time; Path loss factor equals to $\gamma_p = 3.5$ and the variance of shadowing is $z_k = 8$ dB. The channel between the users and the BS is assumed to be block fading. It keeps unchanged from one block to another. All transmitted data are modulated using 4-QAM scheme. In the following representations, all the BER curves are drawn versus SNR, which is defined as p_u/σ_n^2 , where σ_n^2 is assumed to be unity.

Fig. 3 and Fig. 4 show the BER curves of the aforementioned detectors for $N_r = 64$, $K = 16$, $N_T = 4$ and $N_r = 128$, $K = 32$, $N_T = 4$ antennas. It can be seen from both Fig. 3 and Fig. 4 that when SNR is sufficient high, the proposed detectors remarkably outperform the classical QRD and SQRD ones. Specifically, in Fig. 3, at $BER = 10^{-4}$, the QRD-PGD and SQRD-PGD respectively achieve SNR gains of more than 8 dB and 15.5 dB as compared the MMSE. When compared to the SQRD, the respective SNR gains are approximately 6.5 dB and 14 dB. Among the detectors, the BLAST has the highest performance. It outperforms the SQRD-PGD by about 3.7 dB at $BER = 10^{-4}$, as illustrated in Fig. 3. This is obvious because the BLAST requires a huge computational effort as shown in the next section.

These achievements of proposed detectors can be explained through load factors of the systems. Note, low load factor is equivalent to high degree of freedom and hence BER performance is enhanced significantly. For classical detectors, the load factor given by original system is N/N_r while in

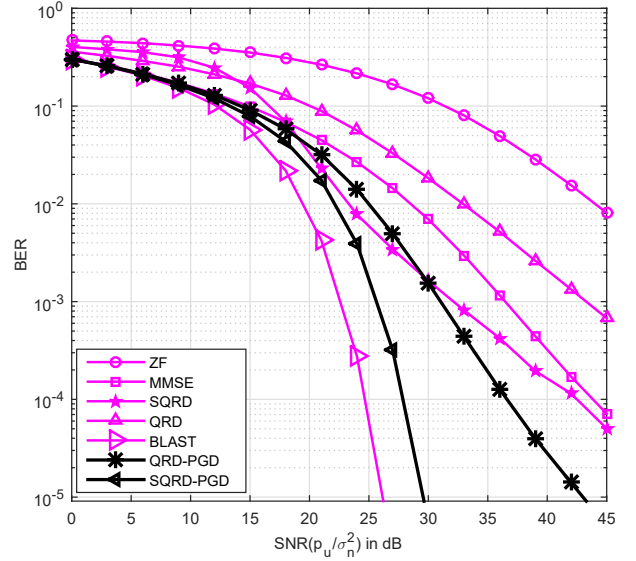


Fig. 3. BER curves versus SNR (dB) of classical ZF, MMSE, QRD, SQRD, BLAST, QRD-PGD and SQRD-PGD detectors when $N_r = 64$, $K = 16$, $N_T = 4$, 4-QAM.

the equivalent load factor of a sub-system in PGD is just $N/(2(N_r + N))$, which is much taller than N/N_r . This means that proposed detectors obtain much higher degree of freedom than those of original ones resulted significant enhancement in their BER performances.

The results from the two figures also demonstrate that at full load condition, i.e., unity load factor, the proposed detectors are able to achieve more SNR gains as the number of antennas increases. For example, the required SNR for the QRD-PGD and SQRD-PGD to obtain at $BER = 10^{-4}$ are respectively about 37 dB and 28 dB when $N_r = N = 64$. The numbers reduce to 35 dB and 25 dB for the case of $N_r = N = 128$ antennas.

V. COMPLEXITY ANALYSIS

In this section, we evaluate the complexities of the proposed detectors as well as the classical ones by counting the required number of floating point operation (Flops) per recovered signal vector. In order to do so, we assume that each real algebraic operation is counted as a flop and the complexities of slicing operation and matrix/vector transposed are ignored [4], [15]. Under the above assumptions, a complex multiplication and a complex division are respectively counted as 6 and 11 flops, while a complex addition or complex subtraction equals 2 flops. Note that multiplying a $m \times n$ matrix by a $n \times l$ one needs to compute total mln multiplications and $ml(n-1)$ additions; an inversion of $m \times m$ matrix requires m^3 multiplications and m^3 additions [16].

It is worth noting that the complexity of a detector can also be computed on the equivalent real system as in [4]. However,

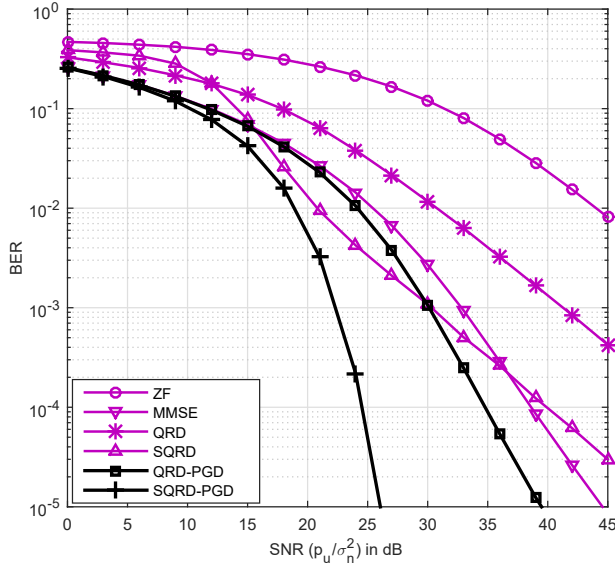


Fig. 4. BER curves versus SNR (dB) of classical ZF, MMSE, QRD, SQRD, QRD-PGD and SQRD-PGD detectors when $N_r = 128$, $K = 32$, $N_T = 4$, 4-QAM.

the complexity evaluated based on the equivalent real system requires higher flops than that based on the complex one [13].

Using above expressions, the complexities of classical ZF, MMSE, QRD, SQRD and BLAST detectors, in terms of flops, are computed to be as follows:

$$C_{ZF} = 8N^3 + 16N^2N_r - 2N^2 + 6NN_r - 2N, \quad (14)$$

$$C_{MMSE} = 8N^3 + 16N^2N_r - 2N^2 + 6NN_r, \quad (15)$$

$$C_{QRD} = 6N^2N_r + 3N^2 + 12NN_r + 4N, \quad (16)$$

$$C_{SQRD} = 6N^2N_r + 5N^2 + 12NN_r + 3N, \quad (17)$$

$$C_{BLAST} = \frac{15}{4}N^4 + 2N^3N_r + N^2N_r^2 + N(16N_r - 2). \quad (18)$$

For the proposed detectors, we can observe that two sub-systems are generated in the same way. Besides, the dimensions of the two sub-systems are equal. Hence, the overall computational cost of proposed detectors is double the complexity of one sub-system. It is also noted that, the required flops for each sub-system include those of generating the sub-system and those of detection process. Therefore, the complexities of proposed detectors are given by:

$$C_{subD-PGD} = 2(C_{Ge} + C_{subD}), \quad (19)$$

herein, $C_{subD-PGD}$ denotes overall complexity of QRD-PGD or SQRD-PGD detector; C_{Ge} and C_{subD} are respectively the complexity of generating a sub-system and that of detection process.

TABLE I
COMPLEXITY COMPARISON

Detector	Number of flops per recovered vector
ZF	$8N^3 + 16N^2N_r - 2N^2 + 6NN_r - 2N$
MMSE	$8N^3 + 16N^2N_r - 2N^2 + 6NN_r$
QRD	$6N^2N_r + 3N^2 + 12NN_r + 4N$
SQRD	$6N^2N_r + 5N^2 + 12NN_r + 3N$
BLAST	$\frac{15}{4}N^4 + 2N^3N_r + N^2N_r^2 + N(16N_r - 2)$
QRD-PGD	$2N^3 + 8N^2N_r + 3aN^2 + \frac{3}{2}N^2 + 8a^2N - 2NN_r + 8aN_rN - 4aN_r + 28aN - 2a + 6N$
SQRD-PGD	$2N^3 + 8N^2N_r + 3aN^2 + \frac{5}{2}N^2 + 8a^2N - 2NN_r + 8aN_rN - 4aN_r + 28aN - 2a + 5N$

*. Note, $N = KN_T$ and $a = N_r + N$

In order to evaluate the complexities, we first represent the channel matrix \mathbf{U}_{ex} as follows:

$$\mathbf{U}_{ex} = \begin{bmatrix} \mathbf{G}^{(1)} & \mathbf{G}^{(2)} \end{bmatrix} = \begin{bmatrix} \mathbf{F}_1 & \mathbf{F}_2 \\ \mathbf{D}_1 & \mathbf{0}_2 \\ \mathbf{0}_1 & \mathbf{D}_2 \end{bmatrix}, \quad (20)$$

where both \mathbf{F}_1 and \mathbf{F}_2 are complex matrices with dimensions of $N_r \times L$, which are generated by taking the first L and the remaining columns of the original channel matrix \mathbf{U} , correspondingly; \mathbf{D}_1 and \mathbf{D}_2 are $L \times L$ diagonal real matrices; $\mathbf{0}_1$ and $\mathbf{0}_2$ are $L \times L$ zero matrices, $L = N/2$.

Let $a = N_r + N$, the complexity C_{Ge} is evaluated to be:

$$\begin{aligned} C_{Ge} &= C_{\mathbf{A}^{(1)}} + C_{\mathbf{G}^{(1)}} + C_{\mathbf{y}^{(1)}} \\ &= N^3 + 4N^2N_r + 4a^2N + N - NN_r + 4aNN_r \\ &\quad - 2aN_r + 8aN - a \text{ (flops)}. \end{aligned} \quad (21)$$

Since the dimensions of each sub-system is $(N_r + N) \times L$, the complexity of applying the QRD or SQRD detector to each sub-system can be extended easily from equation (16) and (17) by replacing N_r and N respectively by $a = N_r + N$ and $L = N/2$. Thus, we get:

$$C_{subQRD} = \frac{3}{2}aN^2 + \frac{3}{4}N^2 + 6aN + 2N \text{ (flops)}, \quad (22)$$

$$C_{subSQRD} = \frac{3}{2}aN^2 + \frac{5}{4}N^2 + 6aN + \frac{3}{2}N \text{ (flops)}. \quad (23)$$

Once C_{Ge} , C_{subQRD} and $C_{subSQRD}$ are determined, the total complexities of proposed detectors are obtained by replacing properly (21), (22) and (23) to (19). The complexities of the detectors under consideration are summarized as in Table I.

The results in Table I show that the complexities of the proposed detectors are proportional to the 3rd order of N , i.e., $O(N^3)$, which are the same as those of linear detectors. Shown in Fig. 5 the complexities of the detectors as $N_r = N$ varies in the range of [60, 200] antennas. The results demonstrate that the proposed detectors have much smaller the complexities than the BLAST, particularly when the number of antenna increases, thereby making the propose more practical. It can also be seen that the computational costs of the QRD-PGD and SQRD-PGD are almost the same to those of linear detectors when N_r is less than a hundred and the gaps between them slightly increase when N_r increases. The higher

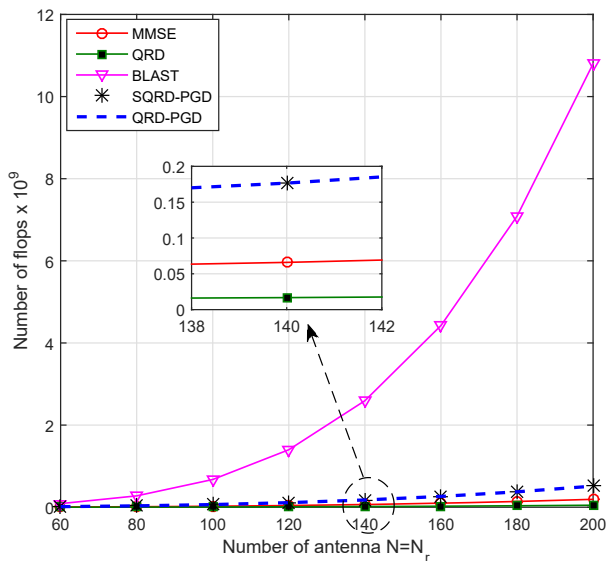


Fig. 5. Complexity curves versus number of antenna when $N = N_r = [60, 200]$.

computational costs of proposed detectors are rewarded by a huge enhancement in BER performance as shown in Section IV.

VI. CONCLUSION

In this paper, we have proposed the so-called PGD algorithm, the QRD-PGD and SQRD-PGD detectors for signal recovery in Massive MIMO systems. Numerical and simulation results show that the proposed detectors significantly outperform their conventional counterparts, such as MMSE, QRD, and SQRD, at comparable detection complexities. Although they still suffers from noticeable performance degradation as compared to the BLAST, they have much lower detection complexities, particularly when the system size increases. Thus, they are potential candidates for signal detection in high load Massive MIMO systems.

REFERENCES

- [1] T. L. Marzetta, "Massive mimo: an introduction," *Bell Labs Technical Journal*, vol. 20, pp. 11–22, 2015.
- [2] H. Q. Ngo, *Massive MIMO: Fundamentals and system designs*. Linköping University Electronic Press, 2015, vol. 1642.
- [3] T. L. Marzetta, E. G. Larsson, H. Yang, and H. Q. Ngo, *Fundamentals of Massive MIMO*. Cambridge University Press, 2016.
- [4] T.-B. Nguyen, T.-D. Nguyen, M.-T. Le, and V.-D. Ngo, "Efficiency zero-forcing detectors based on group detection for massive mimo systems," in *Advanced Technologies for Communications (ATC), 2017 International Conference on*. IEEE, 2017, pp. 48–53.
- [5] R. T. Kobayashi, F. Ciriaco, and T. Abrão, "Efficient near-optimum detectors for large mimo systems under correlated channels," *Wireless Personal Communications*, vol. 83, no. 2, pp. 1287–1311, 2015.
- [6] E. Björnson, E. G. Larsson, and T. L. Marzetta, "Massive mimo: Ten myths and one critical question," *IEEE Communications Magazine*, vol. 54, no. 2, pp. 114–123, 2016.
- [7] B. Hassibi, "A fast square-root implementation for blast," in *Signals, Systems and Computers, 2000. Conference Record of the Thirty-Fourth Asilomar Conference on*, vol. 2. IEEE, 2000, pp. 1255–1259.
- [8] A. Chockalingam and B. S. Rajan, *Large MIMO systems*. Cambridge University Press, 2014.
- [9] J. W. Choi and B. Shim, "New approach for massive mimo detection using sparse error recovery," in *Global Communications Conference (GLOBECOM), 2014 IEEE*. IEEE, 2014, pp. 3754–3759.
- [10] H. Q. Ngo, E. G. Larsson, and T. L. Marzetta, "Energy and spectral efficiency of very large multiuser mimo systems," *IEEE Transactions on Communications*, vol. 61, no. 4, pp. 1436–1449, 2013.
- [11] T. Li, S. Patole, and M. Torlak, "A multistage linear receiver approach for mmse detection in massive mimo," in *Signals, Systems and Computers, 2014 48th Asilomar Conference on*. IEEE, 2014, pp. 2067–2072.
- [12] L. Bai and J. Choi, *Low complexity MIMO detection*. Springer Science & Business Media, 2012.
- [13] R. T. Kobayashi, F. Ciriaco, and T. Abrão, "Efficient near-optimum detectors for large mimo systems under correlated channels," *Wireless Personal Communications*, vol. 83, no. 2, pp. 1287–1311, 2015.
- [14] D. Wubben, R. Bohnke, J. Rinas, V. Kuhn, and K.-D. Kammeyer, "Efficient algorithm for decoding layered space-time codes," *Electronics letters*, vol. 37, no. 22, pp. 1348–1350, 2001.
- [15] T.-D. Nguyen, X.-N. Tran, T.-M. Do, V.-D. Ngo, and M.-T. Le, "Low-complexity detectors for high-rate spatial modulation," in *2014 International Conference on Advanced Technologies for Communications (ATC 2014)*. IEEE, 2014, pp. 652–656.
- [16] G. H. Golub and C. F. Van Loan, *Matrix computations*. JHU Press, 2012, vol. 3.